


Design of a RFID System for Real-Time Tracking of Laboratory Animals

Zwivhuya Romeo Ramudzuli¹ · Reza Malekian¹  · Ning Ye²

Published online: 2 February 2017
© Springer Science+Business Media New York 2017

Abstract In this paper, a real-time RFID system capable of tracking laboratory animals is designed and implemented. Four passive RFID tags based on low frequency are designed and implemented. The tags can be read by any RFID reader that operates on the low frequency range 125–134 kHz. The tags are designed through the investigation of various antenna, encoding, modulation, and energy harvesting techniques. The tag receives the electromagnetic signal via the antenna, and converts it to a DC signal that the micro-controller can use to manipulate the electromagnetic signal with the data such that the reader can decode the unique tag identifier. RFID sensors are designed and implemented to collect data from various monitored areas of a semi natural environment. The data is sent to a central data coordinator for pre-processing and middleware for data error checking, display and storage. The RFID system can successfully detect and store movement data in real time. A read range of 14.5 cm is achieved.

Keywords Radio frequency · Receiving antennas · RFID tags · Transponders · Wireless sensor networks

Zwivhuya Romeo Ramudzuli and Reza Malekian have contributed equally to this work.

✉ Reza Malekian
reza.malekian@up.ac.za

Zwivhuya Romeo Ramudzuli
zwivhuya.ramudzuli@gmail.com

Ning Ye
yening@njupt.edu.cn

¹ Department of Electrical, Electronic and Computer Engineering, University of Pretoria, Pretoria 0002, South Africa

² Department of Computer Science and Technology, Nanjing University of Posts and Telecommunications, Nanjing, China

1 Introduction

In earlier times, data has been collected by specially trained observers [1]. The observers manually collected data as they sat in front of cages. These observers are well trained in behavioural biology and can identify 50 behavioural and movement patterns [2]. Constant human surveillance method of observation introduces various forms of influences to the animal's behaviour and hence the data collected. The tracking performance of the human observers is limited to the individual's concentration span and other constituents such as mood and exhaustion [2, 3].

The problem addressed in this paper is to develop an RFID based animal tracking solution for collecting real-time movement data. In concept, the solution would eliminate the need for extensive human intervention by allowing long-term continuous tracking and data collection for animal behaviour analysis.

Animal behaviour analysis requires long-term collection of movement data. The constituents of behaviour mainly environmental bias includes housing conditions, and the human observer [1], thus it is important that any tracking method used does not significantly influence any of the above mentioned. Presently available laboratory animal tracking methods include the p-Chip, machine vision and the single photon emission computed tomography (SPECT) systems. According to [4], the p-Chip is an implant based light-activated tag designed to operate within line of sight of a laser operated reader. Due to the reading distances of just 1–3 mm, a human operator must hold mice and illuminate the area on which the tag is implanted to get a reading. According to [5], the machine vision system was used to visually monitor insect colonies. A small tray of insects is monitored by a camera. The system can count a number of insects and track them across the bounding box but cannot distinguish an individual insect from the other. According to [6], the SPECT system tracked mice by using high resolution imaging systems. One of the two techniques in SPECT required markers to be placed on the mice and the other laser profiling was used to detect mice moving across a bridge between cages. The SPECT system successfully characterised the mice but did not distinguish them from the other. The proposed RFID system seeks to minimise human interactions during test subjects monitoring and accurately identify each test subject uniquely. Behavioral information such as the animals expression towards the environment and other animals can be studied.

2 Related Works

In an RFID-based animal data recording system presented by [7] [8], a human observer placed an RFID reader within 1 cm of the area on the animal on which the tag is attached by an observer. This approach influences the animals' behaviour and is therefore not suitable for animal behaviour analysis. In [2], the RFID reader was placed in strategic locations in a semi natural environment with a detection range of only 0.5 cm. In [9], clusters of antennas with a detection range of only 1 cm were placed in a 12 cm × 12 cm matrix to partition an area within which mice were studied. All the four approaches including those in [4–6] leave a gap for the present work. The use of short range RFID systems require large number of RFID hardware, accumulate substantial cost and limit the size of the study population. In the system proposed in this paper, the RFID tracking system eliminated the need for manual data collection, uniquely identifies the test subjects and reduced the influence on animal behaviour during data collection, reduced the number

of RFID hardware required. The system can also be employed in other application such as asset inventory management, access control, location systems and health care [10].

The RFID system obtained movement data by recording all RFID tag data as the tags moved across various locations in the semi natural environment. The semi natural environment within which the laboratory animals were kept contained a number of RFID tag readers. Laboratory animals need to be kept in an environment within which they can move around, exercise, and interact with other animals with sufficient space that is clean and undisturbed. A physical model that simulated a semi natural environment with movable objects simulating laboratory animals is built and used to test the prototype. The tag readers interrogated and retrieved the unique tag data as a means of identification.

The unique RFID tag code, reader location code and RFID event time stamp are recorded in a relational database in real time. The database contained data about when (date and time), where (the tag reader code) and who (the tag code) is at the location. Middleware software is developed in order to convert the data into tracking information, resolving reader collisions and ensuring bad reads are eliminated. Once the data is analysed, the results are presented in a user interface on a personal computer and be fed to a webserver to enable users to remotely observe the tracking information.

3 System Overview

The RFID system enables movement tracking of laboratory animals for behaviour analyses. The RFID tracking system was based on the architecture illustrated in Fig. 1.

The RFID management subsystem includes the inputs to the system in the form of RFID tag IDs and their associated readers, wireless transceiver modules, indicator LEDs, voltage regulators, and circuitry that interfaces the reader and the wireless transceiver. The RFID tag design is based on low frequency (LF) to comply with ISO standard 11784 and 11785 [11]. The ISO standards allocated the frequency range of 125–134 kHz for the use of applications such as animal identification. Using the low frequency range offers a number of advantages such as the signals ability to penetrate through objects with high liquid content like mice with less attenuation, communication is least affected by metallic objects [12] and costs the least as compared to equivalent systems on higher frequencies [13].

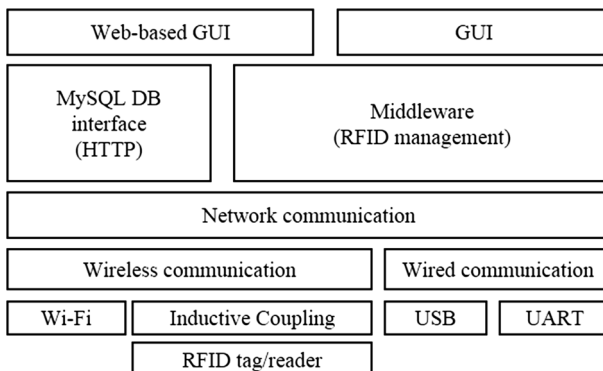


Fig. 1 Architecture of the RFID animal tracking system

4 System Design

4.1 Hardware Development

The RFID tag consisted of a number of components that include the antenna, memory, microcontroller unit (MCU) power supply, data encoder, and modulator. A functional diagram of a typical RFID tag is given in the Fig. 2.

The unique ID is stored on the microcontrollers program memory. The rectifier rectified the AC signal from the antenna into a DC signal. The voltage regulator kept the voltage signal below 3.3 V to protect the microcontroller from excessive voltage as the tag moved closer to the reader. The RFID sensor subsystem can be summarised in the following functional flow diagram.

From Fig. 3, the sensor nodes consisted of a reader, wireless transmitter and power supply. The reader interrogated any RFID tag within its vicinity. When the tag is successfully read, the reader transmitted the data to the wireless transmitter via a serial interface. The transmitter forwards the data to the server subsystem as illustrated in Fig. 4.

The data coordinator subsystem served as a server to which all end devices transmitted all RFID data to. This subsystem consisted of the Wi-Fi transceiver, a human machine interface (HMI) interface with a power button, an LCD and LEDs, 32-bit RISC microcontroller and a USB to Serial adapter. The subsystem displayed the ID of the most recently read tag and the area within which it was detected.

From Fig. 5, the data processing and storage system consisted of the middleware and database. The middleware software stored and analysed the datasets it received from the data coordinator. Statistical information about the objects was derived from the data to build an archive of behavioural information.

4.2 Passive RFID Tag Circuit Design

The passive RFID tag circuit has a network of components that form the passive tag. The tag consisted of a number of sub section which include the antenna, matching capacitor, full-wave rectifier, smoothing capacitor, voltage regulator and modulator.

4.2.1 Antenna Design

The antennas used in the RFID tags are made from copper enamel wire with a diameter of 0.315 mm. The copper material property is chosen since it has a very high permeability [1]. The inductance value for which the antennas are designed is determined using Eq. 1.

The Q factor of a resonant circuit is the measure of the voltage and current step-up at its resonant frequency. The circuit damping ratio can be simply calculated as the reciprocal of the Q factor ($1/Q$). For a desired read range, there is an optimal inductance L_2 , and load

Fig. 2 Functional diagram a typical RFID tag

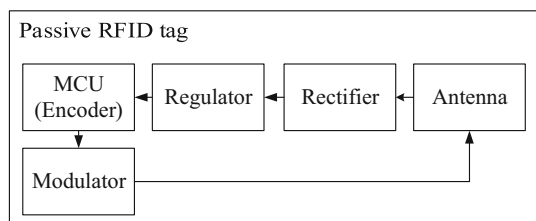


Fig. 3 Functional flow diagram of the RFID sensor subsystem

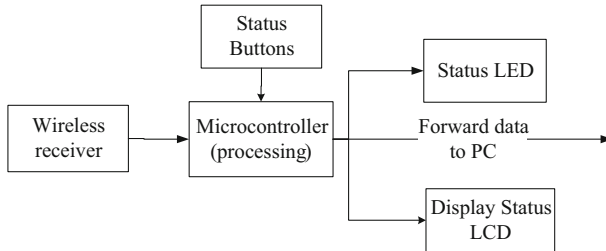
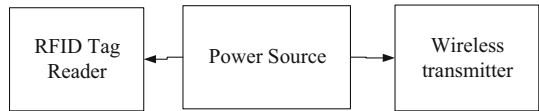
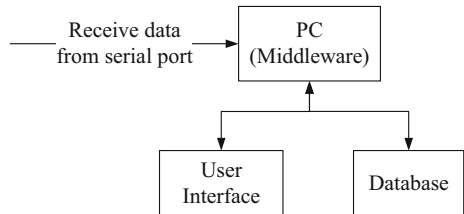


Fig. 4 Functional flow diagram of the data coordinator subsystem

Fig. 5 Functional flow diagram of the data processing and storage subsystem



resistance R_L for the receivers' resonant circuit such that the Q factor is at its maximum. At the optimal inductance L_2 , the RFID tag is considered to operate at its maximum performance. The Q factor for a resonant conductor loop is expressed as [12]:

$$Q = \frac{1}{\frac{R_2}{\omega L_2} + \frac{\omega L_2}{R_L}}, \tag{1}$$

where L_2 denotes the antenna inductance, R_2 is the antenna internal resistance, and ω is the resonant frequency.

Two common antenna shapes will be investigated, namely the circular and square shape. According to a simulation of Eq. 3 done in the mathematical analysis software package Matlab, the optimal inductance of an RFID with a load resistance of 1.650 kΩ is simulated to be 50.78 μH. The load resistance R_L can be calculated using ohms law. For a voltage drop of 3.3 V and a load current of 2 mA, the load resistance is calculated to be 1.650 kΩ. The Fig. 6 shows the optimal Q factor response of a load resistance $R_L = 1.650$ kΩ.

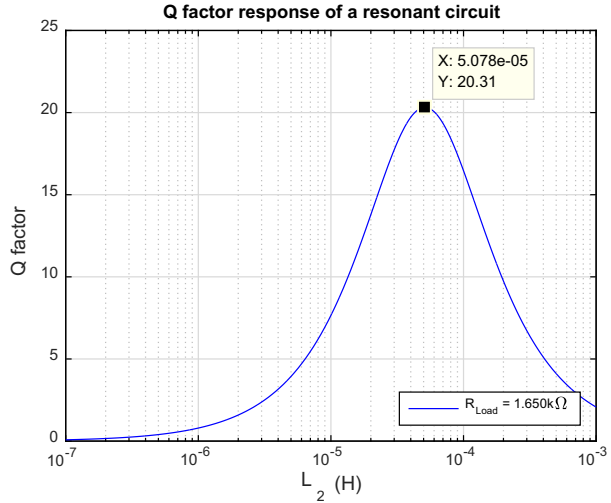
According to [13], the inductance of a square antenna loops with multiple turns is expressed as:

$$L = 0.008 \cdot a \cdot N^2 \cdot \left[2.303 \log_{10} \left(\frac{a}{b+c} \right) + 0.2235 \left(\frac{b+c}{a} \right) + 0.726 \right] \mu\text{H} \tag{2}$$

where N is the number of loop turns, a is the size of the square measured to the centre of the cross section in cm, b is the winding length in cm and c is the winding depth in cm.

The inductance of a circular antenna loops with multiple turns is expressed as:

Fig. 6 The optimal Q factor response of a load resistance $R_L = 1.650 \text{ k}\Omega$



$$L = \frac{0.31(a \cdot N)^2}{6 \cdot a + 9 \cdot h + 10 \cdot b} \mu\text{H}, \tag{3}$$

where N is the number of loop turns, a is average loop radius in cm, b is the winding thickness in cm and h is the winding height in cm.

4.2.2 Matching Capacitor

The antenna forms a resonant circuit that is designed to operate at the carrier frequency of the reader. To optimise the resonant circuit, a matching capacitor is required to form an RLC circuit. The resistor in the equivalent RLC circuit is the antennas internal resistance. Given the antennas inductance, the matching capacitor is calculated using Eq. 4. The Fig. 7 shows the equivalent resonant circuit of the RFID tags antenna.

$$f = \frac{1}{2\pi\sqrt{L_2 \cdot C_2}} \tag{4}$$

Solving for C_2 :

$$C_2 = \frac{1}{(2\pi \cdot f)^2 \cdot L_2} \tag{5}$$

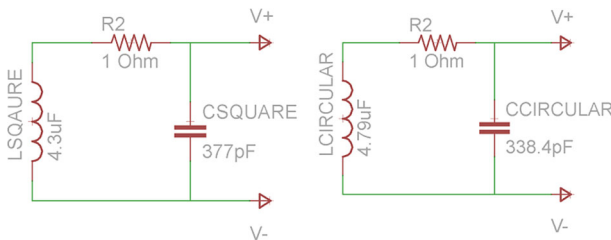


Fig. 7 The equivalent resonant circuit of the RFID tags antenna

4.2.3 Full Wave Rectifier

Once the antenna is designed to receive the RF signal from the reader at the carrier frequency, the AC voltage signal is converted into a DC voltage signal. To achieve this, the full-wave rectifier diode configuration is used to reduce the DC voltage ripple. To further reduce the combined voltage, drop across the full-wave voltage rectifier, Schottky small signal rectifier diode are used. The full-wave rectifier used a total of four diodes of which only two are active per RF signal period. The signal experienced a combined voltage drop of two diodes. Regular rectifier diodes such as the 1N4007s have a combined voltage drop of 1.4 V ($0.7 \text{ V} \times 2$), whereas the ST BAT42 Schottky diodes have a combined voltage drop of 0.52 V (0.26×2). The full-wave rectifier circuit is illustrated in the Fig. 8 below.

4.2.4 Smoothing Capacitor

The rectified output signal from the rectifier is not suitable to provide operational energy to the microcontroller because the signal has considerably high AC component referred to as the ripple. The rectified signal is still an AC signal and needed to be converted to a DC signal which the microcontroller can use to operate. To achieve this, a smoothing capacitor is used to reduce the voltage ripple and improve the load regulation. The maximum current consumed by the tag is chosen as 250 mA. The maximum ripple voltage is chosen to be $\pm 0.5 \text{ V}$ to allow for a 2% maximum ripple. The carrier frequency from the reader is measured to be 127.5 kHz.

$$V_{\text{ripple}} = \frac{I_{\text{load}}}{2f_0 C_{\text{smooth}}}, \quad (6)$$

where V_{ripple} is the maximum ripple voltage, I_{load} is the maximum current drawn by the load, f_0 is the carrier frequency, and C_{smooth} is the smoothing capacitor value. Solving Eq. 6 for the smoothing capacitor value:

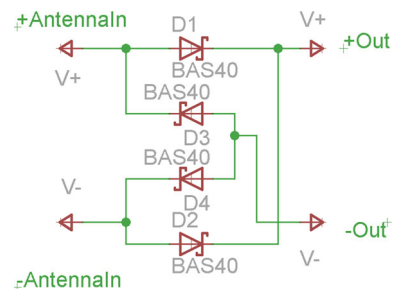
$$C_{\text{smooth}} = \frac{I_{\text{load}}}{V_{\text{ripple}} \cdot 2f_0}, \quad (7)$$

$$C_{\text{smooth}} = \frac{250 \times 10^{-3}}{0.5 \cdot 2 \cdot 125 \times 10^3}$$

$$C_{\text{smooth}} = 2\mu\text{F}$$

The smoothing capacitor circuit is illustrated in the Fig. 9 below.

Fig. 8 The schematic of the full-wave rectifier circuit



4.2.5 LDO Voltage Regulator

The passive RFID tag received the high RF signal as it moved within close proximity of the reader. This high signal produced a high DC signal that could potentially damage the microcontroller on the tag. A voltage regulator is used to keep the DC signal from exceeding the microcontrollers maximum operational supply voltage. The LDO voltage regulator is used as it allowed for a large input DC voltage range -0.3 V to 30 V to maintain an output voltage of 3.3 V . The Fig. 10 shows the schematic of the LDO voltage regulator circuit.

4.2.6 Encoding

The RFID tag used the Manchester encoding. Manchester encoding has an added benefit in that it always yields an average DC level of 50% [15]. This has positive results in the readers' demodulation circuit as it allows better management of the received RF spectrum after modulation. The encoded bit-stream is made up of 64 bits that are divided into five groups of information [15]. The first group of information consisted of 9 header bits. These are a total of nine bits programmed as 1's and are used to inform the reader that data is about to be sent. The second group of information consisted of 10 row parity bits $P[0..9]$. The parity rows use even parity determined from each nibble of the 10 data nibbles. The third group of information is the 10 data nibbles of which only 1 nibble is used at a time represent a single character of the tag ID. A 4-bit hexadecimal value can represent a value from 0×0 to $0 \times F$. The fourth group of information was the 4-bit column parity bits $P[0..3]$. Each bit of the nibbles is the even parity of the data bits column $N_{xy}[0..3]$. The fifth group of information is a single stop bit $S0$ always programmed as a '0'. The tag sent this bit to the reader to alert end of data stream. These 64 bits are transmitted serially and the sequence repeated continuously until the tags power went off. Table 1 shows the 64-bit data setup using the Manchester encoding.

The 64 cycle per bit Manchester encoding scheme is used. The sub-carrier frequency can be calculated by the expression [15]:

$$f_{\text{sub-carrier}} = \frac{f_{\text{carrier}}}{64}, \tag{8}$$

where $f_{\text{sub-carrier}}$ is the sub-carrier frequency, and f_{carrier} is the carrier frequency. The carrier frequency of the low frequency RFID system is assumed 125 kHz. This frequency is given by the ISO 11784/5 standard for animal tracking applications [11].

Fig. 9 The schematic of the smoothing capacitor circuit

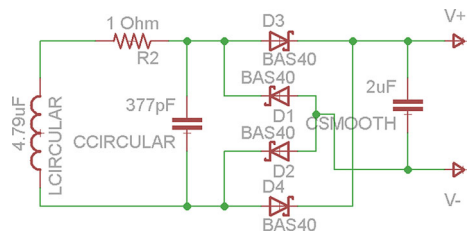


Fig. 10 The schematic of the LDO voltage regulator circuit

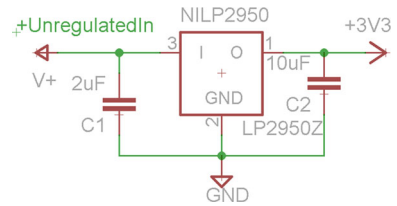


Table 1 The 64-bit data stream using Manchester encoding

1	1	1	1	1	1	1	1	1	1	1	9 header bits	
10 data nibbles					N ₀₀	N ₀₁	N ₀₂	N ₀₃	P0	10 even row parity bits		
					N ₁₀	N ₁₁	N ₁₂	N ₁₃	P1			
					N ₂₀	N ₂₁	N ₂₂	N ₂₃	P2			
					N ₃₀	N ₃₁	N ₃₂	N ₃₃	P3			
					N ₄₀	N ₄₁	N ₄₂	N ₄₃	P4			
					N ₅₀	N ₅₁	N ₅₂	N ₅₃	P5			
					N ₆₀	N ₆₁	N ₆₂	N ₆₃	P6			
					N ₇₀	N ₇₁	N ₇₂	N ₇₃	P7			
					N ₈₀	N ₈₁	N ₈₂	N ₈₃	P8			
					N ₉₀	N ₉₁	N ₉₂	N ₉₃	P9			
					P0	P1	P2	P3	S0			
					Even column parity nibble							

$$f_{\text{sub-carrier}} = \frac{125 \times 10^3}{64} = 1.953 \text{ kHz}$$

$$f_{\text{sub-carrier}} \approx 2 \text{ kHz}$$

The 64 cycles per bit Manchester encoding scheme is chosen to ensure better accuracy of the delays implemented in the microcontroller to achieve a sub-carrier frequency of 2 kHz. Higher sub-carrier frequencies require highly accurate software delays. Manchester encoding states that a transition occurs in the middle of every bit. This implies that at every half period of the sub-carriers' frequency, a transition occurs. The mid bit time can be calculated by the expression [14]:

$$T_{\text{mid-bit}} = \frac{\left(\frac{1}{f_{\text{sub-carrier}}}\right)}{2}, \tag{9}$$

where $f_{\text{sub-carrier}}$ is the sub-carrier frequency and $T_{\text{mid-bit}}$ is the mid bit time or half the period of the sub-carrier frequency.

$$T_{\text{mid-bit}} = \frac{\left(\frac{1}{2 \times 10^3}\right)}{2} = \frac{500 \times 10^{-6}}{2} = 250 \mu\text{s}$$

4.2.7 Modulation

To embed the data signal into the carrier frequency the incident signal from the reader is mixed with the microcontroller signal. To achieve this, a modulating circuit is required. To induce a high current on the tags antenna, the modulation circuit used in the design consisted of one Bipolar Junction Transistor (BJT) and a load resistor configured as a common collector amplifier. The emitter current of a practical common collector amplifier can be expressed as:

$$\Delta I_C = \frac{\Delta V_E}{R_E} = \frac{\Delta V_B}{R_E}, \tag{10}$$

$$V_B = V_E + 0.6$$

where I_C is the collector current, V_E is the emitter voltage, V_B is the base voltage and R_E is the load resistor. A microcontroller with a minimum operation voltage of 1.8 V implies that the BJT's base terminal voltage $V_B = 1.8$ V.

$$V_E = V_B - 0.6$$

$$V_E = 1.8 - 0.6 = 1.2V$$

The emitter load resistance is calculated using Eq. 10 as:

$$I_C = \frac{V_E}{R_E}$$

Let $I_C = 2$ mA

$$R_E = \frac{V_E}{I_C} = \frac{1.2}{2 \times 10^{-3}}$$

$$R_E = 600 \Omega$$

The nearest standard resistor value is 560 Ω . $\therefore R_E = 560 \Omega$

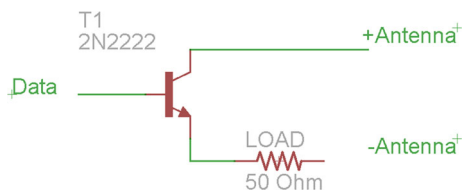
The modulator schematic circuit is illustrated in Fig. 11.

4.2.8 Integrated Schematic

The complete passive RFID tag schematic with all the integrated component is illustrated in Fig. 12.

Four passive tags are designed. Figure 13 shows two of the passive RFID tags. The other tags vary by antenna size for both shapes. Figure 14 shows a size comparison between the designed and commercial RFID tag.

Fig. 11 The schematic of the RFID tag modulator



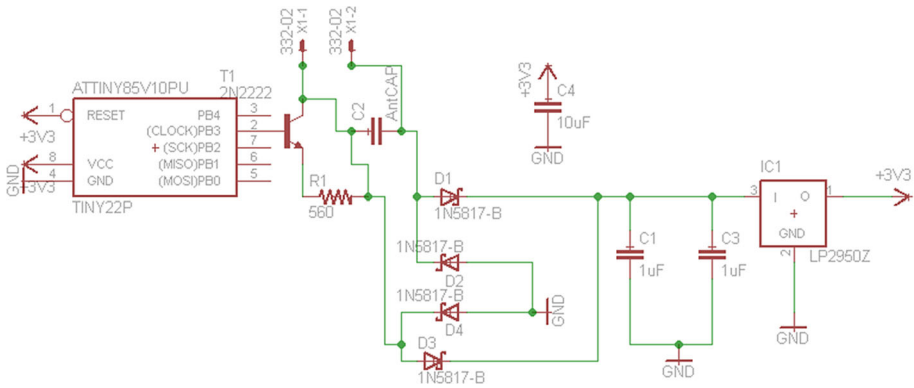


Fig. 12 The complete passive RFID tag schematic

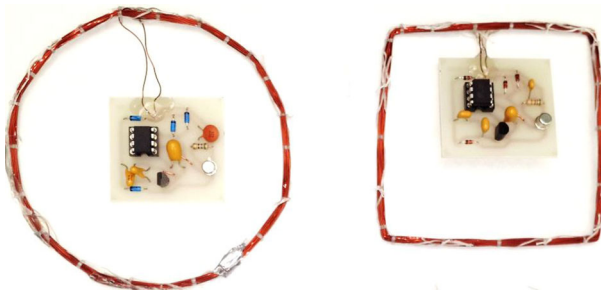


Fig. 13 Two RFID tags of different sizes and shapes



Fig. 14 The relative size comparison of an off the shelf and the designed RFID tag

4.3 High Level System Communication

The RFID tracking system used a star network of Wi-Fi transceivers. The sensor nodes sent the data to the server devices that acted as the access point. The device consisted of the

RFID tag reader, Wi-Fi transceiver, and voltage regulation circuitry. The reader interrogated any tag within its near field and transmits the RFID data to the server node.

The server node in Fig. 15 pre-processes the datasets and forwarded them to the PC. The device consisted of a Wi-Fi transceiver configured as an access point, an 8 bit microcontroller programmed as a serial to USB converter, and a 32 bit microcontroller programmed as a data pre-processor and LCD driver. The device displayed the most recent detected tag identifier and the area within which it is detected in real-time. The same data is forwarded to the middleware where it is further processed, displayed and stored.

One of the three sensor nodes is designed with the Internet of Things (IoT) model. An additional microcontroller was used to configure the Wi-Fi transceiver such that it used the already existing institutions Wi-Fi network and sent a valid HTTP header request with the tag ID to the webserver. This eliminates the need for additional data coordinator devices and PC based middleware software. With the advancements of web technologies, data mining algorithms can be used to produce statistical information. Other web based monitoring services such as IP based video monitoring can be seamlessly integrated with the RFID system. This provides a platform independent system that is accessible to virtually any IP based system. Figure 16 shows a data coordinator/access point device.

4.4 Semi Natural Environment

A computer-aided design (CAD) of the semi natural environment (SNE) is shown in Fig. 17. The model consisted of a $0.75\text{ m} \times 0.9\text{ m} \times 0.1\text{ m}$ maze with three main areas. The green sphere on the figure represents an object with an RFID tag moving across the semi natural environment and the red objects represent an RFID tag reader on each area. The objects location is monitored as it moved across the model. The readers are placed such that they faced the entrances of the partitioned areas in the SNE such that their magnetic fields do not overlap to ensure distinct successful tag readings are obtained in each area. More readers can be used to cover all areas of the SNE if needed. The Fig. 18 shows a prototype of the semi natural environment.

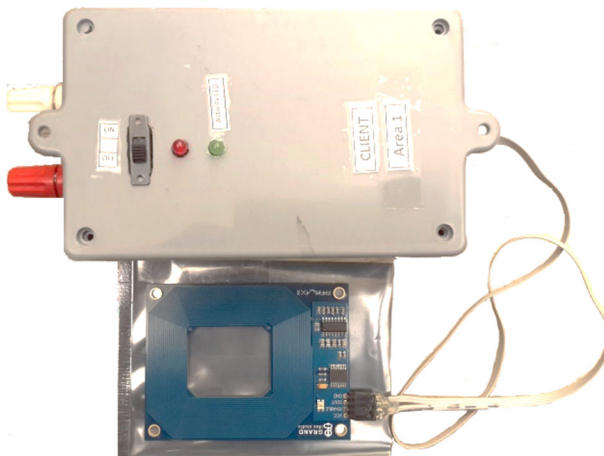


Fig. 15 RFID sensor device



Fig. 16 Data coordinator/Access point device

Fig. 17 A CAD model of the semi natural environment

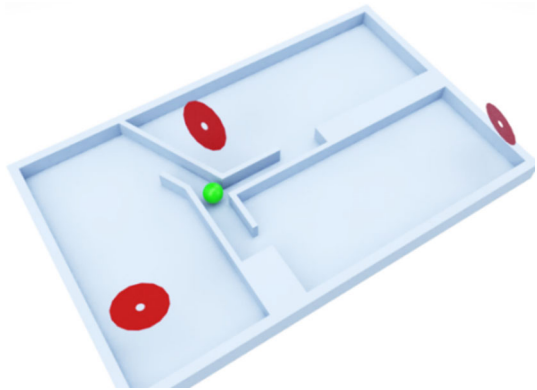


Fig. 18 A prototype of the semi natural environment

4.5 Software Development

The RFID animal tracking system software is divided into three sections. The first section, namely the middleware is responsible for processing the RFID data, displaying statistical information in the form of a GUI and uploading the data to the webserver via an HTTP request.

The RFID tag used Manchester encoding to embed data in the subcarrier signal. Each of the 64 bits are transmitted serially and the process repeats until all bits are encoded. The software flow diagram of the RFID tag is shown in the Fig. 19.

The microcontroller on the RFID tag continuously transmitted the data until it ran out of power. The tags carrier frequency can be expressed by [16]:

$$f = \frac{1}{2\pi\sqrt{L_2 \cdot C_2}} \tag{11}$$

where C_2 also referred to as the antenna tuning capacitor and L_2 is the antennas inductance.

The second section, namely the encoding of data from the RFID tags [17, 18] microcontroller to produce the unique tag IDs. The middleware software flow diagram is illustrated in Fig. 20.

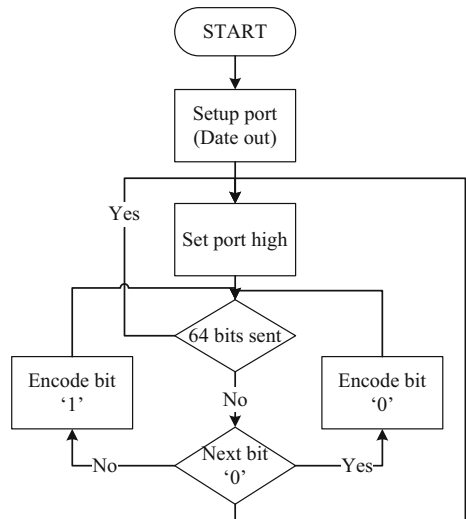
When the user added a list of RFID tag ID to the whitelist, they are stored and used as a filter criterion to eliminate bad reads, and nose generated tag IDs. The MySQL database access credentials are stored and used to gain access to the webserver and return data back to the GUI. The serial communication credentials provided by the user are used by the middleware to use the USB interface to obtain the datasets.

The third section, namely the webserver is responsible for storing the data and making it accessibly to remote devices with internet access capability in the form of HTML pages.

Shown below are the screen shots of the GUI and web application showing the real-time RFID data [19, 20] from the database in Figs. 21 and 22.

The identifier, area, date and time at which the tag is detected is stored and displayed autonomously in real-time.

Fig. 19 The software flow diagram of the RFID tag



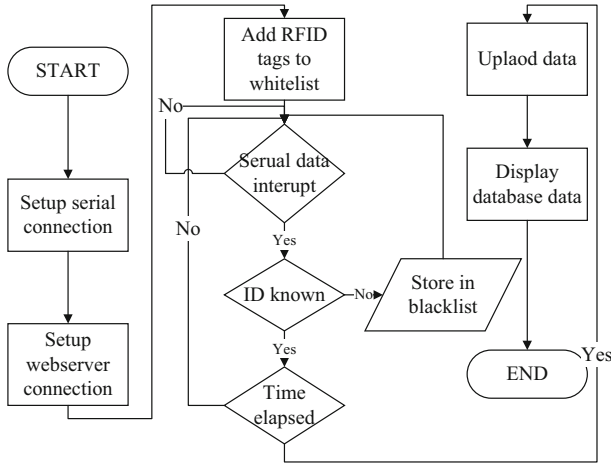


Fig. 20 The software flow diagram of the RFID tracking system middleware

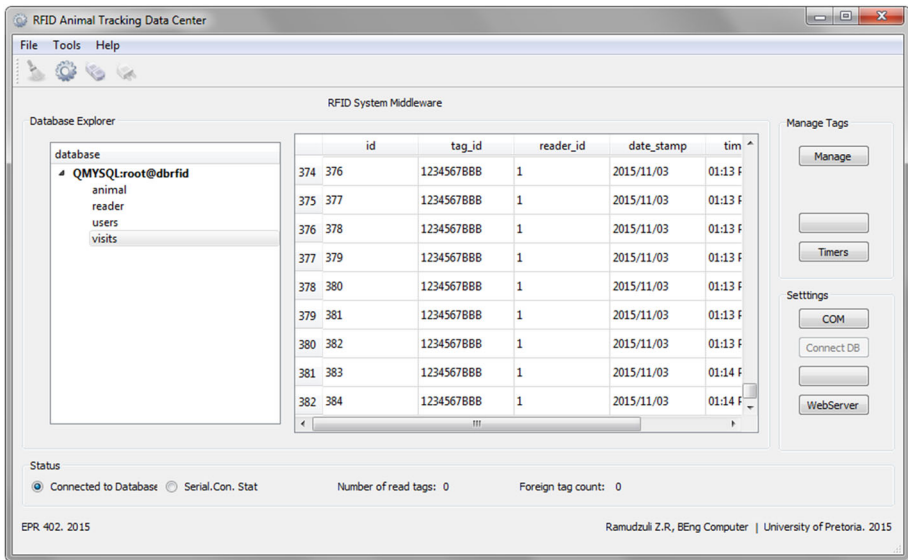


Fig. 21 An image of the GUI main window

5 Results

In order to determine the timeliness of the tracking system, the objective of the first experiment is to measure the amount of time it took to store the RFID tag ID from the time it was read by the reader. Below is a table with part of the movement datasets exported into a comma separated values (CSV) file and tabulated in Table 2.

The objective of the second experiment is to measure the RFID tags operational frequencies in order to determine whether the passive RFID tags complied with the design

Tag ID	Date	Time
1234567AAA	2015-10-21	14:46:06
1234567BBB	2015-10-21	14:46:42
1234567AAA	2015-10-21	14:54:29
1234567AAA	2015-10-21	15:16:47
1234567BBB	2015-10-21	15:23:20
1234567AAA	2015-10-21	15:48:04

Fig. 22 Web application showing the RFID datasets observed on a designated area of the semi natural environment

Table 2 Passive RFID tags inductance, capacitance and carrier frequency summary

Id	Tag_id	Area_id	Date	Time
73	1234567AAA	3	2015/10/21	16:24:44
74	1234567AAA	3	2015/10/21	16:25:11
75	1234567BBB	1	2015/11/02	16:15:09
76	1234567CCC	1	2015/11/02	16:15:22
77	1234567BBB	2	2015/11/02	16:15:31
78	1234567BBB	1	2015/11/02	16:15:33

frequency of 125–134 kHz. The frequency responses of the tags were measured and the results tabulated in Table 3.

The frequency response of the tags antenna during data transmission is given in Fig. 23. The figure contains artefacts of a square wave signal due to the process of amplitude modulation. The reader uses an envelope detector circuit to detect amplitude variation of its magnetic field to decode the data from the tag. The tag does not transmit its own electromagnetic field; it manipulates the electromagnetic signal transmitted by the reader to transmit its data.

The objective of the third experiment is to measure the maximum read distance and power of the passive RFID tag. The maximum measured read distances for the different tags were measured and tabulated in Table 4.

Figure 24 illustrates the setup of the experiment. The reader and tag are attached to a support frames, and the separation distance is increased and measured until the maximum readable distance is reached for each tag. The maximum read distance can be significantly reduced depending on the tags relative physical orientation to the reader, presence of RF obstruction between the tag and reader, and crosstalk between multiple tags.

Table 3 Passive RFID tags inductance, capacitance and carrier frequency summary

Tag ID	Inductance (μH)	Matching capacitance (μF)	Carrier frequency (kHz)
1234567AAA	121.8	12.79	126.544
1234567BBB	237.1	6.676	126.596
1234567CCC	291.9	5.423	126.578
1234567DDD	200.04	7.987	126.571

Fig. 23 FFT of the passive RFID tag with ID 1234567AAA

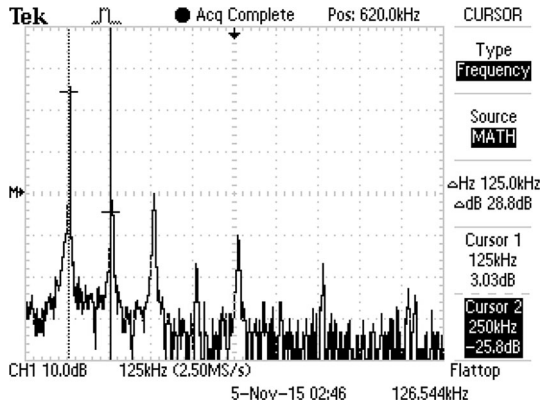


Table 4 Passive RFID tag maximum read distance summary

Tag	Tag ID	Maximum read distance (cm)	Antenna shape	Antenna area (cm ²)
1	1234567AAA	14.5	Square	100
2	1234567BBB	13.7	Circular	78.54
3	1234567CCC	11.4	Circular	113.1
4	1234567DDD	11.6	Square	64



Fig. 24 Maximum read distance experiment setup. On the left is a passive RFID tag, a ruler in the middle, and a reader on the right

The received power by the different tags are compared in the graph in Fig. 25.

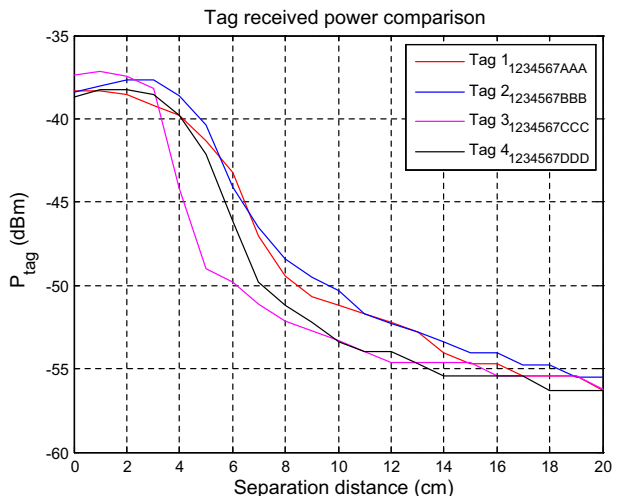
According to Fig. 25, the received power decreased exponentially with an increase in separation distance. Tags associated with smaller antennas received the largest amount of power at the readers near field but were unable to receive sufficient operational power over a larger separation distance. Tags associated with large antennas received slightly lower power at the readers near field but maintained larger operational power over a larger distance compared to tags with smaller antennas. Other parameters such as the antennas effective resistance, inductance, capacitance and orientation affected the tags performance. The power efficiency can be expressed by Eq. 12.

$$\eta_{tag} = \frac{P_{tag}}{P_{reader}} \tag{12}$$

The power and efficiency curves will be similar because efficiency is calculated as the ratio of the receiver and constant transmitter power, hence the curve would scale by the factor equal to the transmitter power. According Fig. 25, the square antenna loop (Tag 1) performed better than the circular loop (Tag 2). The length of the square loop is equal to the diameter of the circular coil. The square antenna loop (Tag 4) with a length of 8 cm performed better than a circular loop (Tag 3) with a diameter of 12 cm. Smaller antenna tags had high power efficiency over a short distance of 7.5 cm. Large antenna tags would maintain higher power efficiency over a longer distance compared to smaller antenna tags. Tag 1's antenna performed better than the other tags and had the least internal resistance and inductance compared to the other tag antennas.

The test for RFID system timeliness confirmed that movement data could be obtained and stored on average within 1 s. This was essential in ensuring that subsequent data could be obtained and stored with least delay. The RFID system effectively captured datasets across all areas. The delay could be reduced by improving the readers decoding time during tag detection. The test for the RFID tag frequencies confirmed that the low frequency design complied with the ISO 11784 and 11785 standards [11]. The average carrier frequency for all the tags was 126.57 kHz and confirms it is possible to design various antennas for a similar carrier frequency. This frequency can be matched to the readers' carrier frequency of 127.5 kHz by designing the antennas such that the required tuning

Fig. 25 The figure compares the received power of the four passive RFID tags



capacitor is of a standard value. A maximum read distance of 14.5 cm was achieved after evaluating various antenna designs and optimising key parameters such as resistance, inductance, size, shape and orientation. The GUI successfully logged and exported all movement data.

6 Future Works

Energy scavenging circuit design in passive RFID tags remains a major area of study. Since the passive tag depends on the readers' electromagnetic field to operate, efficiency and miniaturisation of energy harvester is critical to improving the read range. To further optimise the tag antenna, printed antennas can be studied for tag miniaturisation. The microcontroller used on the tag contributes to the high energy consumption and therefore other data carrying mechanism need to be considered. An increase in reader carrier bandwidth could increase the detection performance by providing tolerance for tag to reader carrier frequency mismatch. The use of readers with larger external antennas can significantly increase the transmitted electromagnetic field, and subsequently miniaturise the tags as a smaller antenna area is sufficient for the desired longer read ranges.

The use of IoT in data collection can provide more effective ways to measure, collect, analyse and present behavioural statistics. The availability of large amount of movement data introduces a challenge in algorithms required to generate useful information.

7 Conclusion

A low frequency RFID animal tracking and behaviour analysis system has been proposed and validated. The tracking subsystem consist of passive RFID tags designed and implemented from first principles. The RFID sensor devices placed in various areas of the semi natural environment use a dedicated Wi-Fi network to transmit data to the data coordinator device that pre-process the data. The LF RFID readers were positioned on the walls of the matrix such that the radiation region is in the vicinity of the entrances of each matrix area. This configuration allowed a single reader to monitor multiple entrances. The detection rate was improved since the tags were designed for long read ranges for the given reader. The behaviour analysis software platform consists of a middleware and web application that generates statistical information from the collected datasets. It is able to collect, process, display, and store the reading data in real time. The resonant frequency of the tags varies from the readers' carrier frequency by approximately 0.784%. The tag performance is least affected since the deviation is minimal. All the tags comply with the ISO 11784 and 11785 standards. A maximum read distance of 14.5 cm distance was achieved after evaluating various antenna designs and optimising key parameters such as antenna resistance, inductance, size, shape and orientation. The proposed system demonstrates the appropriateness in enabling effective animal tracking and behaviour analysis based on LF RFID technology.

Acknowledgements This work was supported in part by the National Research Foundation of South Africa, Research Development Program by the University of Pretoria as well as National Natural Science Foundation of P. R.

References

1. Wang, K., Diet, A., Chakra, S. A., Conessa, C., Grzeskowiak, M., Bouaziz, T., Protat, S., Delcroix, D., Rousseau, L., Lissorgues, G., and Joisel, A. (2012). Detecting range and coupling coefficient tradeoff with a multiple loops reader antenna for small size RFID LF tags, in *2012 IEEE International Conference on RFID-Technologies and Applications (RFID-TA)*, pp. 154–159.
2. Wahlsten, D., Metten, P., Phillips, T. J., Boehm, S. L., Burkhart-Kasch, S., Dorow, J., et al. (2003). Different data from different labs: Lessons from studies of gene-environment interaction. *Journal of Neurobiology*, *54*, 283–311.
3. PharmaSeq. (2013). *Tagging of laboratory mice using p-Chip*. New Jersey: PharmaSeq.
4. Balch, T., Khan, Z., & Veloso, M. (2001). *Automatically tracking and analyzing the behavior of live insect colonies*. Montreal, Quebec: AGENTS.
5. Goddarda, J. S., Gleasona, S. S., Kerekesa, R. A., Paulusa, M. J., Smithb, M. F., Weisenbergerb, A. G., and Welchb, B. (2003). Two methods for tracking small animals in SPECT imaging, in *SPIE-The International Society for Optical Engineering*, Bellingham, Washington, pp. 129-139.
6. Farid, Z., Nordin, R., and Ismail, M. (2013). Recent advances in wireless indoor localization techniques and system. *Journal of Computer Networks and Communications*, *2013*, 1–11.
7. Voulodimos, A. S., Patrikakis, C. Z., Sideridis, A. B., Ntakis, V. A., & Xylouri, E. M. (2010). A complete farm management system based on animal identification using RFID technology. *Computer and Electronics in Agriculture*, *70*(2), 380–388.
8. Samad, A., Murdeshwar, P., & Hameed, Z. (2010). High-credibility RFID-based animal data recording system suitable for small-holding rural dairy farmers. *Computer and Electronics in Agriculture*, *73*(2), 213–218.
9. Kritzler, M., Lewejohann, L., Krger, A., Raubal, M., and Sachser, N. (2006). An rfidbased tracking system for laboratory mice in a semi-natural environment, in *Pervasive 2006 Workshop Proceedings*. Dublin, Ireland.
10. Ozguven, E. E., & Ozbay, K. (2015). An RFID-based inventory management framework for emergency relief operations. *Transportation Research Part C: Emerging Technologies*, *57*, 166–187.
11. Iso.org, 'ISO 11785:1996—Radio frequency identification of animals—Technical concept', 2015. [Online]. Accessed Nov 08, 2015, from http://www.iso.org/iso/iso_catalogue/catalogue_tc/catalogue_detail.htm?csnumber=19982.
12. Klaus, F., & Handbook, R. F. I. D. (2003). *Fundamentals and applications in contactless smart cards, radio frequency identification and near-field communication* (3rd ed.). New Jersey: Wiley.
13. Lehpamer, H. (2008). *RFID design principles* (1st ed., pp. 133–201). Massachusetts: Artech House, Incorporated.
14. Youbok, L. (2003). *Antenna circuit design for RFID applications* (pp. 1–50). Arizona: Microchip Technologies Incorporated.
15. Prescott, T. (2009). Manchester Coding Basics Application Note. *Techniques*, p. 24. www.atmel.com.
16. Lee, Y., & Sorrells, P. (2004). *microID® 125 kHz RFID system design guide*. Arizona: Microchip Technology Incorporated.
17. Wang, Z., Ye, N., Malekian, R., Xiao F., Wang, R. (2016). TrackT: Accurate tracking of RFID tags with mm-level accuracy using first-order Taylor series approximation. *Ad Hoc Networks*, *53*, 132–144.
18. Malekian, R., Moloisane, N.R., Nair, L., Maharaj, B.T., Chude-Okonkwo, U.A.K. (2014). Design and Implementation of a Wireless OBD II Fleet Management System. *IEEE Sensors Journal*, *17*(4), 1154–1164.
19. Malekian, R., Kavishe, A.F., Maharaj, B.T., Gupta, P.K., Singh, G., Waschefort, H. (2016) Smart vehicle navigation system using hidden Markov model and RFID technology. *Wireless Personal Communications*, *90* (4), 1717–1742.
20. Jin, X., Shao, J., Zhang, X., An W., Malekian, R. (2016) Modeling of nonlinear system based on deep learning framework. *Nonlinear Dynamics*, *84*(3), 1327–1340.



Zwivhuya Romeo Ramudzuli received the B.E. degree in computer engineering from the University of Pretoria, Pretoria, South Africa, in 2015. He is currently pursuing the M.E. degree in computer engineering. He is a Junior Engineer with the Square Kilometre Array South Africa (SKA SA), National Research Foundation. His research interests include radiofrequency identification system design, telescope signal processing, and high performance computing (HPC).



Reza Malekian is an Associate Professor with the Department of Electrical, Electronic, and Computer Engineering, University of Pretoria, South Africa. His research interests include advanced sensor networks, Internet of Things, and mobile communications and intelligent transportations. Dr. Malekian is also a Chartered Engineer, a Professional Member of the British Computer Society and an associate editor for the IEEE Internet of Things Journal as well as lead guest editor for a special issue titled “Internet of Things and Sensors Technologies for Intelligent Transportation Systems” in IEEE Transactions on Intelligent Transportation Systems.



Ning Ye received Ph.D. degree from the Institute of Computer Science from Nanjing University of Post and Telecommunications, China, in 2009. In 2010, Dr. Ning worked as Visiting Scholar and Research Assistant in the Department of Computer Science, University of Victoria, Canada. She is currently a professor at Nanjing University of Post and Telecommunications, China. She is also a senior membership of CCF and a member of pervasive computing specialty committee in China. Her research focuses on the security and information processing, Advanced Sensor Technologies and intelligent transportation. She is a guest editor for a special issue titled “Internet of Things and Sensors Technologies for Intelligent Transportation Systems” in IEEE Transactions on Intelligent Transportation Systems and “Cyber-physical systems and context-aware sensing and computing” in Computer Networks, Elsevier..